







# Personalized Image Recoloring for Color Vision Deficiency Compensation

Zhenyang Zhu , Masahiro Toyoura , *Member, IEEE*, Kentaro Go , Kenji Kashiwagi ,  
Issei Fujishiro , *Senior Member, IEEE*, Tien-Tsin Wong, *Member, IEEE*, and Xiaoyang Mao , *Member, IEEE*

**Abstract**—Several image recoloring methods have been proposed to compensate for the loss of contrast caused by color vision deficiency (CVD). However, these methods only work for dichromacy (a case in which one of the three types of cone cells loses its function completely), while the majority of CVD is anomalous trichromacy (another case in which one of the three types of cone cells partially loses its function). In this paper, a novel degree-adaptable recoloring algorithm is presented, which recolors images by minimizing an objective function constrained by contrast enhancement and naturalness preservation. To assess the effectiveness of the proposed method, a quantitative evaluation using common metrics and subjective studies involving 14 volunteers with varying degrees of CVD are conducted. The results of the evaluation experiment show that the proposed personalized recoloring method outperforms the state-of-the-art methods, achieving desirable contrast enhancement adapted to different degrees of CVD while preserving naturalness as much as possible.

**Index Terms**—color vision deficiency, recoloring personalization, contrast enhancement, naturalness preservation.

## I. INTRODUCTION

THREE kinds of cone cells, so-called L-cones, M-cones, and S-cones, are distributed on the retina of the human eye and are sensitive to long-, medium-, and short-wavelength visible light, respectively. These cone cells play a critical role in forming the color vision of an individual. However, approximately

200 million people suffer from color vision deficiency (CVD), which is related to abnormalities in cone cells, and no medical cure is available [1]. CVD can be classified as anomalous trichromacy, dichromacy, or monochromacy. Both anomalous trichromacy and dichromacy involve abnormalities of one of the three types of cone cells, while monochromacy involves two or all. In dichromacy, the abnormal cone is assumed to lose its function completely; in anomalous trichromacy, only a part of the function is lost. Both anomalous trichromacy and dichromacy can be classified as protan, deutan, or tritan defects depending on whether the abnormalities occur in the L-, M-, or S-cones, respectively. Protan, deutan, and tritan defects in anomalous trichromacy and dichromacy are named protanomaly, deuteranomaly, tritanomaly, protanopia, deuteranopia, and tritanopia, respectively.

On the one hand, with the rapid development of the Internet and the spread of mobile computing devices, the creation and propagation of multimedia content flourished. Visual multimedia content, such as videos on video sharing sites, pictures posted on social media, well-designed web pages, chromatic charts in worksheets, etc., fills up the private and professional lives of users. People who suffer from CVD may fail to acquire the information contained in these multimedia contents. Considering the large population of people with CVD, adapting the visual contents to perception characteristics of users with CVD is necessary [2]. Several image recoloring methods [3]–[21] have been proposed to compensate for the loss in the ability to discriminate colors. In addition to contrast, the importance of naturalness preservation has also been raised in state-of-the-art image recoloring studies [9]–[17]. Since CVD is congenital, people with CVD are accustomed to their own perception of the colored world. Therefore, when recoloring an image, large changes to the colors that are perceivable by CVD individuals may cause the image to appear “unnatural” to them. Thus, naturalness preservation in CVD compensation can be defined as the preservation of the colors that an individual with CVD can perceive in the original image. In other words, naturalness preservation can be realized by restraining the difference between the CVD simulation results of the original image and the recolored image.

One major problem with existing recoloring methods is that the degree of deficiency is completely ignored. Sharpe *et al.* [1] reported that the incidences of anomalous trichromacy and dichromacy are 5.71% and 2.28% in men, and 0.39% and 0.03% in women, respectively, which indicates that anomalous trichromacy accounts for the majority of CVD. However, all existing

Manuscript received September 6, 2020; revised March 21, 2021; accepted March 24, 2021. Date of publication March 31, 2021; date of current version March 29, 2022. This work was supported by JSPS Grants-in-Aid for Scientific Research, Japan under Grant 17H00738, 20J15406. The associate editor coordinating the review of this manuscript and approving it for publication was Dr. F. Battisti. (*Corresponding author: Xiaoyang Mao.*)

Zhenyang Zhu is with the Graduate School of Engineering, University of Yamanashi, Kofu 400-8511, Japan (e-mail: zhuyamanashi2016@gmail.com).

Masahiro Toyoura, Kentaro Go, and Xiaoyang Mao are with the Department of Computer Science and Engineering, University of Yamanashi, Kofu 400-8511, Japan (e-mail: mtoyoura@yamanashi.ac.jp; go@yamanashi.ac.jp; mao@yamanashi.ac.jp).

Kenji Kashiwagi is with the Department of Ophthalmology, University of Yamanashi, Chuo 409-3898, Japan (e-mail: kenjik@yamanashi.ac.jp).

Issei Fujishiro is with the Department of Information and Computer Science, Keio University, Yokohama 223-8522, Japan (e-mail: fuji@ics.keio.ac.jp).

Tien-Tsin Wong is with the Department of Computer Science and Engineering, The Chinese University of Hong Kong, Shatin, Hong Kong (e-mail: ttwong@cse.cuhk.edu.hk).

This article has supplementary material provided by the authors and color versions of one or more figures available at <https://doi.org/10.1109/TMM.2021.3070108>.

Digital Object Identifier 10.1109/TMM.2021.3070108

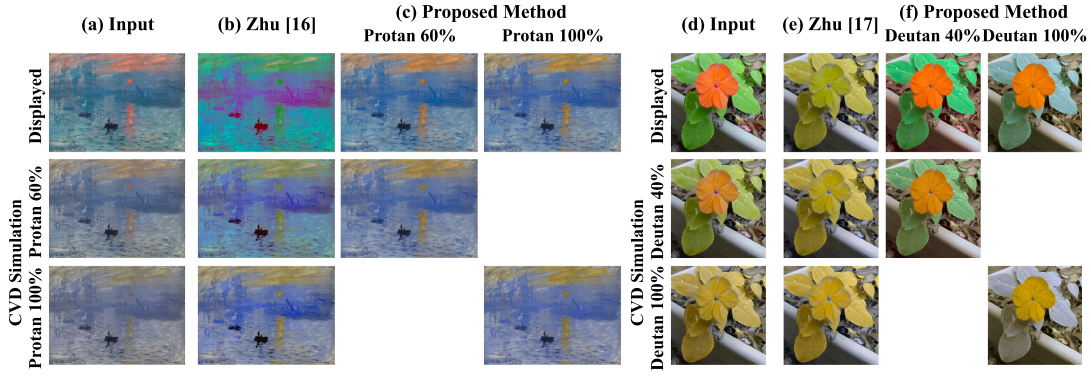


Fig. 1. Comparison of the images produced by Zhu *et al.* [16], [17] and the proposed method for assisting people with different degrees of CVD. (a) and (d): the original images. (b): recoloring result of Zhu *et al.* [16]. (e): recoloring result of Zhu *et al.* [17]. (c) and (f): recoloring results of the proposed method.

recoloring algorithms for a single image are based on the computational model of dichromacy and thus may be less effective for anomalous trichromacy. Even for dichromacy, existing methods may fail to achieve the expected effect if they fail to consider the difference in perceivable colors caused by varying degrees of CVD. Fig. 1 shows two examples of such failures with the two most recent recoloring algorithms [16], [17].

Fig. 1(a) compares the image of Claude Monet’s “Impression, sunrise” (Fig. 1(a)-top) and the perception of protan 60% (Fig. 1(a)-middle) and protan 100% (Fig. 1(a)-bottom) obtained with the CVD simulation model proposed by Machado *et al.* [22]. We can see that the contrast between the sun and sky is attenuated in the simulation of protan 60% and is almost lost in that of protan 100%. The recoloring result (Fig. 1(b)-top) of Zhu *et al.* [16] preserves contrast and naturalness well for protan 100% (Fig. 1(b)-bottom), but for protan 60%, the tints of the simulation image (Fig. 1(b)-middle) appear to be quite different from those of the original image (Fig. 1(a)-middle), i.e., the sun and cloud appear greenish compared to the simulation image. Fig. 1(d) compares a picture of a red flower over green leaves (Fig. 1(d)-top) and its CVD simulation of deutan 40% (Fig. 1(d)-middle) and deutan 100% (Fig. 1(d)-bottom). The contrast between the flower and leaves is lost in the simulation of deutan 100% (Fig. 1(d)-bottom). Fig. 1(e)-top is the resulting image recolored by Zhu *et al.* [17]. As can be confirmed in Fig. 1(e)-bottom, the method even fails to enhance the contrast for deutan 100%. We found that this failure is caused by a lack of consideration of the varying degrees of deficiency in perceiving individual colors.

To address the abovementioned problem, this paper proposes a novel personalized recoloring method that adapts contrast enhancement and naturalness preservation based on individual degrees of CVD. The personalized recoloring method improves compensation effects in the following two ways:

- 1) Unlike the existing methods, which are customized for dichromacy compensation, the proposed method makes use of the anomalous trichromacy simulation model to recolor images optimally for all degrees of anomalous trichromacy. Fig. 1(c) demonstrates this advantage of the proposed method. The same quality of compensation can be confirmed for both protan 60% (Fig. 1(c)-left-middle)

and protan 100% (Fig. 1(c)-right-bottom). Note that the proposed method generates different images for the two cases.

- 2) Contrast enhancement and naturalness are two contradictory targets. While existing methods deal with all colors equally, requiring a trade-off between the two targets, the proposed method can automatically resolve this trade-off according to the degree of deficiency in perceiving individual colors. Fig. 1(f) demonstrates a case in which our personalized recoloring can preserve contrast well for both deutan 40% (Fig. 1(f)-left-middle) and deutan 100% (Fig. 1(f)-right-bottom) by trading the changes of unperceivable colors for contrast.

The proposed personalized recoloring is based on an optimization process that compromises between contrast enhancement and naturalness preservation within the color gamut of anomalous trichromacy. While the color gamut of dichromacy is assumed to be planar, that of anomalous trichromacy is a 3D subspace of the color gamut of normal vision. Consequently, we introduce a new optimization model to address the additional color dimension and obtain results adapted to an individual’s CVD degree by solving a nonlinear equation system. To resolve the trade-off between contrast enhancement and naturalness preservation for individual colors according to the CVD degree, a new metric that compares individual colors with their CVD simulation is introduced and embodied in the naturalness preservation constraint. To assess the effectiveness of the proposed method, a quantitative evaluation with common metrics and subjective studies involving 14 volunteers with varying degrees of CVD was conducted. The results of the evaluation demonstrate that the proposed personalized recoloring outperforms the state-of-the-art methods, achieving compensation effects optimized for varying degrees of CVD. The major contributions of this paper can be summarized as follows:

- 1) A novel degree-adaptable recoloring algorithm for CVD compensation simultaneously considers naturalness preservation and contrast enhancement.
- 2) A novel method for automatically resolving the trade-off between contrast enhancement and naturalness preservation for individual colors according to the CVD degree results in an optimal compensation effect.

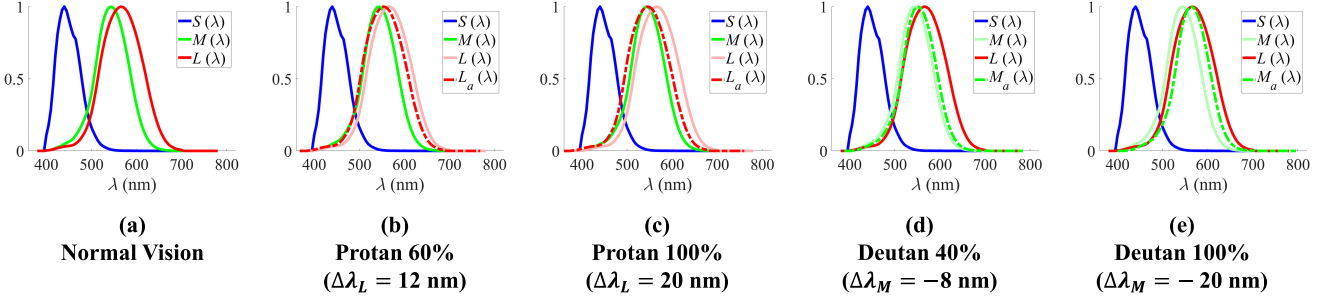


Fig. 2. Spectral sensitivity curves of cone cells of normal vision and those with protan 60% and 100% and deutan 40% and 100%. (a): Sensitivity curves of three types of cone cells of normal vision. (b) curves of cone cells with protan 60%. (c) curves of cone cells with protan 100%. (d) curves of cone cells with deutan 40%. (e) curves of cone cells with deutan 100%.

- 3) A subjective evaluation experiment with 14 volunteers with varying degrees of CVD is conducted to investigate the compensation effects of all state-of-the-art recoloring algorithms as well as that of the proposed personalized recoloring algorithm. The experiment also provides a comparison between the CVD degrees measured by the computation model and traditional clinical CVD tests.
- 4) An application for CVD users is provided to choose the proper CVD degree for the best recoloring result.

The remainder of the paper is organized as follows: Section 2 surveys the related works. Section 3 details the proposed personalized recoloring method. Section 4 describes the evaluation, while section 5 discusses the limitations of the proposed method and potential applications. Section 6 concludes the paper.

## II. RELATED WORK

### A. CVD Simulation

Brettel *et al.* [23] proposed simulating the color perception of dichromats in the LMS color space. The color gamut of dichromats was assumed to be constructed of two half-planes, consisting of neutrals and some common hues, such as yellow and blue. Vienot *et al.* [24] presented a linear transformation method for dichromacy simulation based on [23]. Machado *et al.* [22] adopted a two-stage model [25] and simulated the color perception of anomalous trichromacy and dichromacy based on spectral sensitivity shift theory [1]. According to the two-stage model [25], there are two stages in an individual's perception of a light stimulus: light stimulus to LMS-cone responses and LMS-cone responses to opponent-color space. The spectral sensitivity curves of normal cones are illustrated in Fig. 2(a). Anomaly in the cone cell influences the first stage by causing the sensitivity curve of the corresponding cone to shift (Fig. 2(b)-(e)), but the second stage is the same as for normal cones. Protanomaly occurs because the sensitivity curve of the L-cone is shifted to that of the M-cone (Fig. 2(b) and Fig. 2(c)); deuteranomaly is a result of the curve of the M-cone shifting to that of the L-cone (Fig. 2(d) and Fig. 2(e)). Moreover, the amount of the shift is related to the severity of CVD, with a spectral shift of 20 nm approximately equivalent to dichromacy. In Fig. 2, the degree is quantized as a percentage according to the amount of the curve shift. Protan 60% indicates that the L curve is shifted by 12 nm,

presuming that a shift of 20 nm is equivalent to 100%. Corresponding CVD simulation results can be found in Fig. 1. In this paper, the model in [22] is used to simulate the perceptions of CVD.

### B. Optical Color Filters for CVD

To improve CVD color discriminability, tinted glasses, such as EnChroma [26] and VINO [27], were designed to filter out the visible light of particular spectra. However, a user study conducted by Luis *et al.* [28] showed that EnChroma failed to improve the results of diagnosis tests. Moreover, color filters can change the appearance of unaffected colors [29], especially in the case of VINO glasses.

### C. Recoloring for CVD Compensation

Recoloring algorithms [3]–[8] have been proposed for the purpose of enhancing color contrast for CVD. Huang *et al.* [3] maintained the distance between color clusters when remapping them into the CVD gamut. Rasche *et al.* [4], [5], Wakita *et al.* [6], and Machado *et al.* [7] added a luminance consistency constraint to their optimization models. Lin *et al.* [8] warped the color distribution in the opponent color space [25] for contrast enhancement. However, the deviations from the original image are too great to meet the requirements for naturalness preservation.

For naturalness preservation, some approaches [9]–[15] attempted to minimize deviation from the original image. Hassan *et al.* [9], [10] regarded the difference between the original image and its CVD simulation as a perception error and compensated for it by increasing the blue channel according to the amount of the error. However, the contrast loss in the blue area was severe in their results because the relationship between pixels was not considered. Lau *et al.* [11] segmented the image into several regions using k-means++ [30] and enhanced the contrast in adjacent regions. Huang *et al.* [12] minimized the deviation from the original image and enhanced the contrast of all color pairs. Kuhn *et al.* [13] introduced k-means and uniform quantization image quantization and adopted the mass-spring system for optimization. Huang *et al.* [14], [15] extracted several key colors from images or videos, and then the key colors were remapped for contrast enhancement. In [16], [17], a small number of dominant colors were extracted and recolored within the color gamut of dichromats; for the dominant color extraction,



candidate clusters were iteratively merged through a comprehensive comparison of pixel numbers and distances in the image and color spaces. The previously mentioned naturalness-preserving methods [9]–[17] were all developed based on dichromacy simulation models [23], [24] and achieved favorable effects in dichromacy compensation. However, the subjective experimental results in [16], [17] also revealed the distinct difference in the effects between anomalous trichromats and dichromats. In fact, there are significant differences in the effect depending on the CVD color gamut. In other words, it is very difficult to achieve satisfactory results for varying degrees of CVD if the images are recolored assuming a single CVD degree. Our work is the first to adapt both contrast enhancement and naturalness preservation to the CVD degrees of individuals.

#### D. Processing for Visual Sharing

To enable visual sharing between individuals with CVD and those with normal vision, some studies [18]–[21], [31], [32] sought to preserve the color appearance of the original image as much as possible for people with normal vision while improving the color discrimination for those with CVD. Hung *et al.* [31] and Sajadi *et al.* [32] overlaid different texture patterns on different color regions. Chua *et al.* [18], Shen *et al.* [19], and Hu *et al.* [20], [21] proposed the use of a stereoscopic display to realize visual sharing. In this paper, we propose a recoloring algorithm for CVD compensation that can be applied to conventional monitors, such as personal computer screens, and thus we only compare our method with those for a single image.

#### E. Color Vision Test

A typical clinical color vision test includes an Ishihara test [33], a Farnsworth Panel D15 [34] (Panel D15), a Farnsworth 100 hue test [35] (100-hue test), and an anomaloscope test. Of these, the Ishihara test and Panel D15 are used to diagnose the type of CVD, while the 100-hue test and anomaloscope test can identify the degree of CVD. Although the results of the 100-hue test or anomaloscope test cannot be directly applied to the recoloring algorithms or used to define the color gamut of CVD, we utilized the 100-hue test with our participants as a reference. As one of our major contributions, the results of our subjective experiment also provide insights into the relationship between the CVD degrees measured by a computation model and those from traditional clinical CVD tests. Shen *et al.* [19] developed a color gamut calibration interface based on [22]. A comprehensible discussion about the color vision test is beyond the scope of this paper, but we will discuss the possibilities and limitations of using the test results of Shen *et al.* [19] in the proposed recoloring method.

### III. PROPOSED METHOD

#### A. Background

In [16], [17], recoloring is performed within the color gamut of dichromats. First, the colors in the original image are projected into the color gamut of dichromacy using the method in [23]. To constrain the loss of contrast, the CVD perception of the difference among the recolored colors must be as strong as the

normal vision perception of the differences among the original colors; to constrain the loss of naturalness, changes in the CVD perception must be as small as possible. The objective function is formulated as follows:

$$E = \beta E_1 + E_2, \quad (1)$$

$$E_1 = \sum_{i=1}^N \|SIM(c_i^+) - SIM(c_i)\|_2^2, \quad (2)$$

$$E_2 = \sum_{i=1}^N \sum_{j=1, j \neq i}^N \|SIM(c_i^+) - SIM(c_j^+) - \delta_{ij}\|_2^2, \quad (3)$$

where  $c_i$  and  $c_i^+$  denote the  $i$ th colors in the original image and the recolored image;  $SIM(\cdot)$  denotes CVD simulation operation using the method in [23];  $\|\cdot\|_2$  denotes the L2 norm of a vector; and  $\delta_{ij}$  represents the color contrast between  $c_i$  and  $c_j$  in the original image.  $\beta$  is used to adjust the weights of naturalness preservation and contrast enhancement constraints. Finally, the recoloring is completed by minimizing (1). The results of the subjective experiments in [16], [17] show that the resulting images are not suitable for individuals with anomalous trichromacy. Moreover, as shown in Fig. 1, ignoring the variations in individual color perception may cause the recoloring in [16], [17] to fail to enhance contrast even for dichromacy.

For the CVD simulation model in [22], the spectral sensitivity curves of normal L-, M-, and S-cones, which are shown in Fig. 2, are denoted as  $L(\lambda)$ ,  $M(\lambda)$ , and  $S(\lambda)$ , respectively; the amount of shift in the anomalous L- and M-cones is represented as  $\Delta\lambda_L$  and  $\Delta\lambda_M$ , respectively. Thus, spectral sensitivity curves of anomalous cones can be represented as in [22]:

$$L_a(\lambda) = L(\lambda + \Delta\lambda_L), \quad (4)$$

$$M_a(\lambda) = M(\lambda + \Delta\lambda_M), \quad (5)$$

Then, the cone responses are transformed by a matrix  $T_{LMS2Opp}$  to opponent-color space as follows:

$$\begin{bmatrix} WS(\lambda) \\ YB(\lambda) \\ RG(\lambda) \end{bmatrix}_{pa} = T_{LMS2Opp} \begin{bmatrix} L_a(\lambda) \\ M(\lambda) \\ S(\lambda) \end{bmatrix}, \quad (6)$$

$$\begin{bmatrix} WS(\lambda) \\ YB(\lambda) \\ RG(\lambda) \end{bmatrix}_{da} = T_{LMS2Opp} \begin{bmatrix} L(\lambda) \\ M_a(\lambda) \\ S(\lambda) \end{bmatrix}, \quad (7)$$

where  $pa$  and  $da$  denote protan and deutan defects, and  $WS$ ,  $YB$ , and  $RG$  denote the luminance, yellow–blue, and red–green channels in the opponent-color space, respectively.

Given a stimulus  $c$  in the RGB color space, let  $\Gamma_{\text{normal}}$  denote the transformation matrix mapping  $c$  to the opponent-color space of an individual with normal vision and  $\Gamma$  the matrix calculated from (4) and (6) (or (5) and (7)) for mapping  $c$  to the opponent-color space of a CVD individual; then, CVD simulation can be carried out by:

$$\tilde{c} = \Gamma_{\text{normal}}^{-1} \Gamma c, \quad (8)$$

where  $\tilde{c} = (\tilde{r}, \tilde{g}, \tilde{b})^T$  denotes the CVD simulation result of  $c = (r, g, b)^T$ .  $\Gamma_{\text{normal}}^{-1} \Gamma$  is rewriting as a  $3 \times 3$  matrix, which

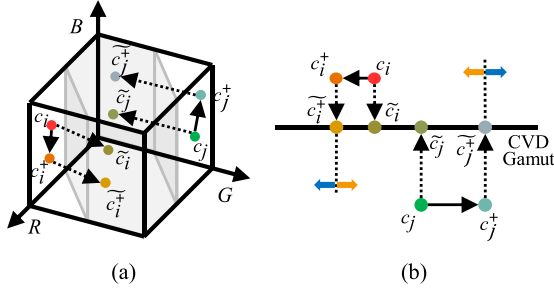


Fig. 3. Recoloring model of the proposed method. (a) The cube represents the color gamut of normal vision, and the space in the shadow indicates the CVD gamut; colors  $c_i$  and  $c_j$  in the original image are perceived as  $\tilde{c}_i$  and  $\tilde{c}_j$  by CVD; with the proposed method,  $c_i$  and  $c_j$  are recolored as  $c_i^+$  and  $c_j^+$ , which are perceived as  $\tilde{c}_i^+$  and  $\tilde{c}_j^+$ , for naturalness preservation and contrast enhancement. (b) Details of the recoloring illustrated in (a). The blue and orange arrows in (b) indicate the constraints of contrast and naturalness, respectively.

is represented as:

$$T = \begin{bmatrix} t_{11} & t_{12} & t_{13} \\ t_{21} & t_{22} & t_{23} \\ t_{31} & t_{32} & t_{33} \end{bmatrix}. \quad (9)$$

Then, the CVD simulation procedure  $\tilde{c} = Tc$  can be written as:

$$\begin{bmatrix} \tilde{r} \\ \tilde{g} \\ \tilde{b} \end{bmatrix} = \begin{bmatrix} t_{11} & t_{12} & t_{13} \\ t_{21} & t_{22} & t_{23} \\ t_{31} & t_{32} & t_{33} \end{bmatrix} \begin{bmatrix} r \\ g \\ b \end{bmatrix}. \quad (10)$$

In this way, perceptions of different degrees of CVD can be simulated by changing the amount of spectral sensitivity curve shift.

### B. Personalized Recoloring Model

This work aims to support CVD individuals by supplying them with recolored images adapted to their degree of deficiency. An optimization scheme equivalent to that described in the Background section is adopted in the proposed method, and recoloring is performed within the color gamut of CVD of a specified degree. The constraints of contrast enhancement and naturalness preservation are included in the recoloring model. The model given in [22] is introduced to simulate CVD perception, and the targeted CVD degree is represented by  $T$ . It should be noted that an important feature distinguishing the proposed method from previous methods [16], [17] is the introduction of  $T$ , which results in a nonlinear optimization model. We developed our own solver, which will be elaborated in the latter part of this section.

Fig. 3 illustrates the recoloring model of the proposed method. First, colors  $c_i$  and  $c_j$  in the color gamut of normal vision are projected into the subspace by multiplying  $T$  with  $c_i$  and  $c_j$  to obtain the CVD simulated colors  $\tilde{c}_i$  and  $\tilde{c}_j$ . The distance between  $\tilde{c}_i$  and  $\tilde{c}_j$  is usually shorter than the distance between  $c_i$  and  $c_j$ , and hence, a loss of contrast occurs. At this point, colors  $\tilde{c}_i$  and  $\tilde{c}_j$  are the most natural to people with CVD. Then,  $c_i$  and  $c_j$  are optimized, as depicted by the simplified 2D illustration in Fig. 3(b). The optimization results and CVD perception of

the results are denoted as  $c_i^+$ ,  $c_j^+$ ,  $\tilde{c}_i^+$ , and  $\tilde{c}_j^+$ , respectively. For contrast enhancement,  $\tilde{c}_i^+$  and  $\tilde{c}_j^+$  are pushed away from each other, but this increases the loss of naturalness. Finally, result factoring in the two targets, contrast enhancement and naturalness preservation, is obtained along with optimized recoloring. The objective function is formulated as follows:

$$E_{pr} = \beta E_{nat} + E_{cont}, \quad (11)$$

$$E_{nat} = \sum_{i=1}^N \alpha_i \|T(c_i^+ - c_i)\|_2^2, \quad (12)$$

$$E_{cont} = \sum_{i=1}^N \sum_{j=1, j \neq i}^N (\|T(c_i^+ - c_j^+)\|_2^2 - \|\delta_{ij}\|_2^2)^2, \quad (13)$$

$$\delta_{ij} = c_i - c_j. \quad (14)$$

In addition to the introduction of  $T$  for adapting the optimization to the CVD degree of individuals, another important contribution of our paper is the introduction of coefficient  $\alpha_i$  to preserve the perceivable colors as much as possible. Our concept is to consider the CVD perception error of individual colors. Hues with a small perception error, such as yellow and blue, should be preserved after recoloring. In other words, colors with smaller perception errors should be set with higher naturalness weights, while those with larger errors should be set with lower weights. Therefore, the coefficient  $\alpha_i$  is adopted to individually control the naturalness weight of a single color, which is calculated as follows:

$$\alpha_i = \exp\left(-\frac{\|Tc_i - c_i\|_2^2}{2\pi\sigma^2}\right) + \varepsilon, \quad (15)$$

where parameter  $\sigma$  normalizes the perception error and is empirically set to 0.2 in the current implementation;  $\varepsilon$  is a small constant so that  $\alpha_i$  does not reach zero.

### C. Implementation

1) *Solver*: While the optimization problems in [16], [17] can be easily solved as linear systems, adapting the degree-varying simulation model leads to a complex nonlinear optimization problem, for which we developed our own solver. In our implementation, a conventional gradient descent method was adopted for the optimization. We partially differentiate with respect to the  $\tilde{c}$  objective function (11) about the resulting color  $c_i^+ = (r_i^+, g_i^+, b_i^+)^T$ . The partial derivative can be calculated as follows:

$$\frac{\partial E_{pr}}{\partial x_i^+} = \beta \alpha_i \omega_x (c_i^+ - c_i)$$

$$+ 2 \sum_{j=1, j \neq i}^N \omega_x (\|T(c_i^+ - c_j^+)\|_2^2 - \|\delta_{ij}\|_2^2) (c_i^+ - c_j^+),$$

$$x \in [r, g, b], \quad (16)$$

$$\begin{cases} \omega_r = t_{11}T_1 + t_{21}T_2 + t_{31}T_3 \\ \omega_g = t_{12}T_1 + t_{22}T_2 + t_{32}T_3 \\ \omega_b = t_{13}T_1 + t_{23}T_2 + t_{33}T_3 \end{cases}, \quad (17)$$

$$\begin{cases} T_1 = [t_{11}, t_{12}, t_{13}] \\ T_2 = [t_{21}, t_{22}, t_{23}] \\ T_3 = [t_{31}, t_{32}, t_{33}] \end{cases}, \quad (18)$$

and the resulting color  $c_i^+$  is updated as follows:

$$c_i^+ \leftarrow c_i^+ + \eta \left[ \frac{\partial E_{pr}}{\partial r_i^+}, \frac{\partial E_{pr}}{\partial g_i^+}, \frac{\partial E_{pr}}{\partial b_i^+} \right]^T, \quad (19)$$

where step length  $\eta = -0.01$ . This procedure is repeated until the solution converges. For natural images, the original image is set as the initial condition.

Because the scale of the system of equations is related to the number of colors, the computational cost can be very high when applying the optimization to all of the colors in the original images. To accelerate the recoloring, we reduce the scale of the system by recoloring some important colors contained in the image and then propagate the recolored colors to the rest of the image. Consequently, recoloring is performed through the following procedure: 1) extract dominant colors from the original image; 2) recolor the extracted dominant colors through optimization guided by (11); and 3) propagate the recolored dominant colors to the whole image, with recolored dominant colors as the propagation source.

2) *Dominant Color Extraction and Recoloring*: Dominant color extraction aims at selecting colors that account for certain numbers of pixels in the input image and are distinguishable from each other. We used the same method as Zhu *et al.* [16] to extract the dominant colors. Most conventional clustering approaches require users to set some parameters in advance, such as the number of clusters in the case of K-means, while Zhu *et al.* [16] succeeded in adapting the parameters to the image content automatically. Their algorithm starts by regarding all colors in the image as candidate dominant colors and then merges similar colors into clusters. During this merging, the pixel number of a color or cluster is regarded as a vital indicator. Distributions of colors or clusters in the image space and their differences in the color space also influence this process.

Throughout the extraction procedure, a variable  $\phi$ , called the radius of similarity comparison, is adopted. Colors or clusters are compared with each other only when they are within  $\phi$  to each other in the color space. The merging procedure is performed in an iterative way, that is, by increasing the radius of comparison step by step. The procedure stops if the number of candidate dominant colors at the current radius is identical to that of the previous radius or if the radius reaches the upper limit  $\phi_{\max} = 100$ . The advantage of using an iterative approach is that the method can adapt to the color ranges of different images. For images with a large color range, a larger radius of comparison is preferred and vice versa. The extracted dominant colors are recolored using (11).

3) *Edit Propagation*: To recolor the entire image, the edit propagation method is employed to diffuse the recolored dominant colors to the whole image. In this study, edit propagation methods [36]–[38] are implemented for comparison. Finally, the result generated by [36] is used in the experiment, as it produces the most satisfactory results. Further discussion will be offered in Section 5.2.

Generally, a user exemplar is required by these edit propagation methods to modify the color appearance of the image. The exemplar can be represented as color pair  $(c_i, s_i)$ , where  $c_i$  denotes a color in the original image and  $s_i$  represents the target color specified by users to  $c_i$ .

Taking into consideration the set of exemplars  $\Omega$  and constraints on neighboring colors  $\Psi$ , the propagation of [36] is formulated as the optimization function as follows:

$$E_{ep} = \gamma \sum_{i \in \Omega} \|z_i - s_i\|_2^2 + \sum_{i=1}^N \|z_i - \sum_{j \in \Psi_i} w_{ij} z_j\|_2^2, \quad (20)$$

where  $z_i$  represents the resulting value of  $c_i$ ,  $\Psi_i$  is a set of colors nearest to  $c_i$ ,  $\gamma$  stands for the weight of the exemplar and is set to 0.1,  $c_j$  is one color in  $\Psi_i$ , and weight  $w_{ij}$  is obtained by computing a locally linear embedding model, which minimizes

$$\sum_{i=1}^N \|c_i - \sum_{j \in \Psi_i} w_{ij} c_j\|_2^2. \quad (21)$$

Exemplars can be reinterpreted as pairs of the original and recolored dominant color and can be substituted into (20). The partial derivative equations of (20) are linear and can be solved using the biconjugate gradient (BiCG) algorithm.

#### IV. RESULTS AND EVALUATION

We conducted qualitative, quantitative, and subjective evaluation experiments to evaluate the effectiveness of the proposed method in terms of contrast enhancement and naturalness preservation. As the three latest state-of-the-art methods considering both contrast enhancement and naturalness preservation for CVD compensation, the recoloring results of Hassan *et al.* [10] and Zhu *et al.* [16], [17] are used for comparison.

##### A. Qualitative Evaluation

Fig. 4 and Fig. 5 use two examples to qualitatively compare the proposed method with the state-of-the-art methods [10], [16], [17]. The first row includes the original images (Fig. 4(a) and Fig. 5(a)), recolored images by [10] (Fig. 4(b) and Fig. 5(b)), [16] (Fig. 4(c) and Fig. 5(c)), [17] (Fig. 4(d) and Fig. 5(d)), and the proposed method for three different degrees (Fig. 4(e) and Fig. 5(e)). Simulations of CVD 20%, 60%, and 100% for those images are shown in the 2nd, 3rd, and 4th rows, respectively.

Fig. 4(a) shows that the contrast between the sun and sky is attenuated when the degree of CVD increases. We find that none of the three existing methods succeeds in both contrast enhancement and naturalness preservation for all three different degrees of CVD, whereas the proposed method can generate an image with sufficient contrast as well as the least color deviation from the simulation image for each of the three degrees of CVD. For the recoloring result of [10] (Fig. 4(b)), the sun is indistinguishable from the sky in the simulation of protan 100%. For the images resulting from [16] (Fig. 4(c)) and [17] (Fig. 4(d)), the simulation of protan 100% shows that it is easier to distinguish the sun from the sky compared to the original images in Fig. 4(a); however, especially for [16] (Fig. 4(c)), the deviations of colors from the simulations of the original image are more obvious



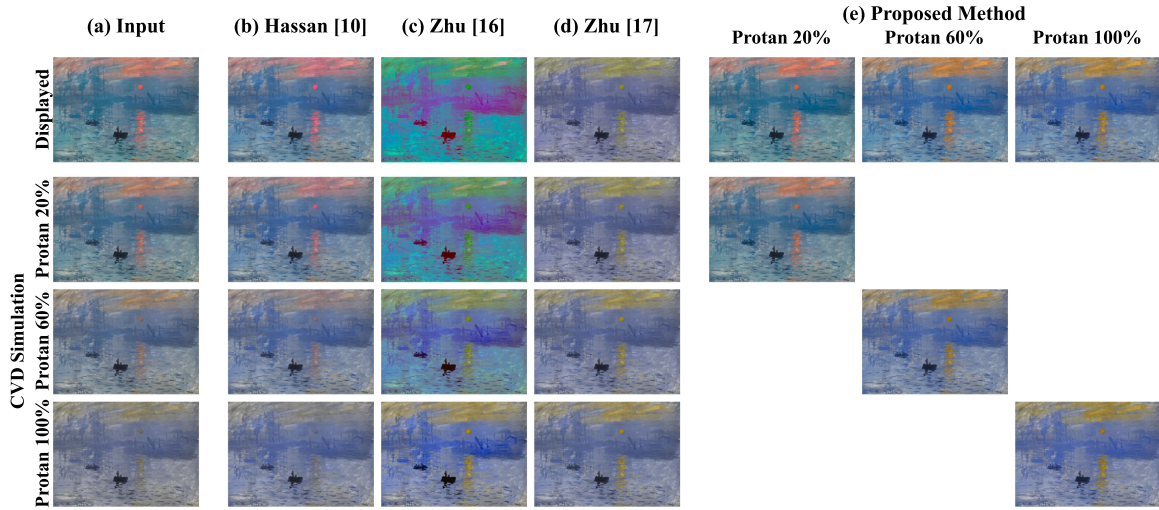


Fig. 4. Comparison of the recoloring results of Hassan *et al.* [10], Zhu *et al.* [16], [17], and the proposed method for protan defects. (a) The original image and its CVD simulation results. (b)-(d) Recoloring results of Hassan *et al.* [10] and Zhu *et al.* [16], [17]. (e) Recoloring results of the proposed method for protan defects of 20%, 60%, and 100%. Images in the first row are the original and recoloring results. Simulation results of protan 20%, 60%, and 100% are shown in the second, third, and fourth rows, respectively.

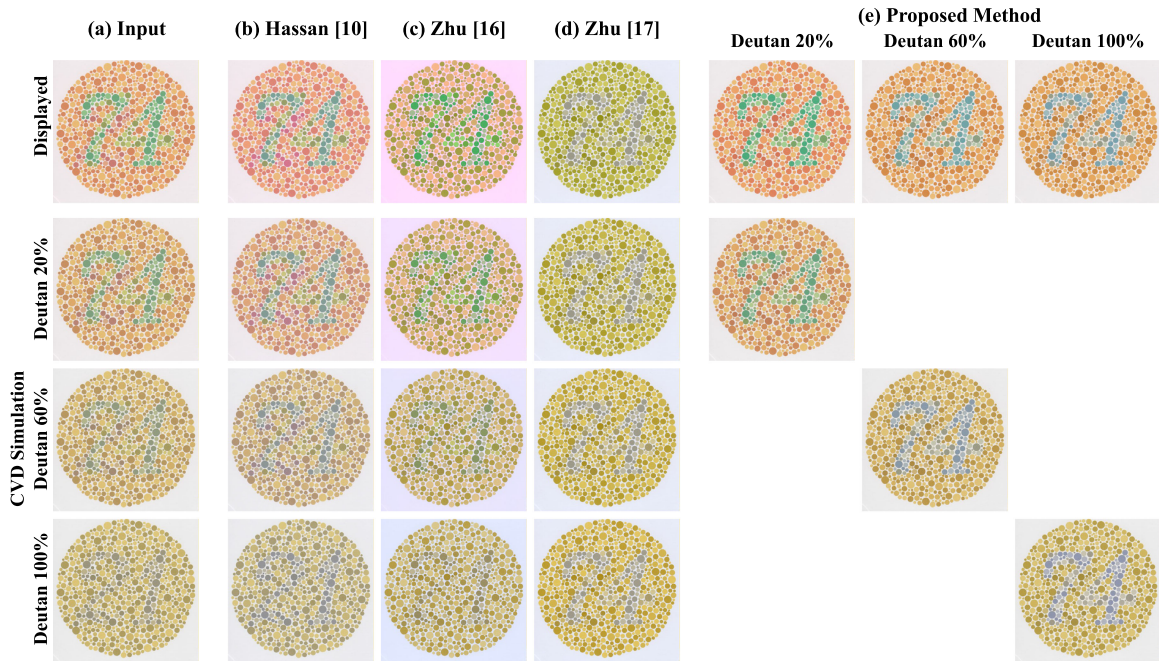


Fig. 5. Comparison of the recoloring results of Hassan *et al.* [10], Zhu *et al.* [16], [17], and the proposed method for deutan defects. (a) The original image and its CVD simulation results. (b)-(d) Recoloring results of Hassan *et al.* [10] and Zhu *et al.* [16], [17]. (e) Recoloring results of the proposed method for deutan defects of 20%, 60%, and 100%. Images in the first row are the original and recoloring results. Simulation results of deutan 20%, 60%, and 100% are shown in the second, third, and fourth rows, respectively.

when the degree of CVD is reduced, which means that those results may appear to be unnatural to people with anomalous trichromacy. For the proposed method (Fig. 4(e)), the recoloring results for degrees 20%, 60%, and 100% are presented; the contrast between the sun and sky is enhanced for each degree, while the color deviation from the simulations of the original image is minimal.

Fig. 5(a) shows that people with CVD may have difficulty reading figures in the Ishihara test charts because the contrast between figures and the background is lost. For [10]

(Fig. 5(b)), [16] (Fig. 5(c)), and [17] (Fig. 5(d)), CVD simulations reveal that the recolored charts fail to enhance the discriminability of the figures. Fig. 5(e) shows that the discriminability of the figures is enhanced by the proposed method, while the perceived color changes from the simulation of the original image are minimal.

To evaluate the performance of the proposed method, quantitative and subjective experiments were conducted, and the results were compared with those using existing methods [10], [16], [17].

TABLE I  
AVERAGE LOSS OF NATURALNESS OF ELEVEN RESULTING IMAGES SYNTHESIZED BY THE FOUR METHODS AND EVALUATED WITH THE SIMULATIONS OF CVD 20%, 40%, 60%, 80%, AND 100% (A LOWER VALUE INDICATES A BETTER RESULT)

Type	Degree	Hassan [10]	Zhu [16]	Zhu [17]	Proposed Method					
					$\beta=0.1$		$\beta=0.2$		$\beta=0.3$	
					Without $\alpha$	With $\alpha$	Without $\alpha$	With $\alpha$	Without $\alpha$	With $\alpha$
Protan	20%	10.55	30.52	18.74	<b>5.58</b>	5.61	<b>4.79</b>	5.74	<b>4.31</b>	4.36
	40%	10.70	23.37	14.72	<b>8.06</b>	<b>7.62</b>	<b>6.23</b>	7.06	<b>5.39</b>	5.55
	60%	10.78	17.44	12.10	<b>9.94</b>	<b>9.64</b>	<b>7.47</b>	8.20	<b>6.23</b>	6.51
	80%	10.83	12.98	10.83	<b>10.78</b>	<b>10.60</b>	<b>7.89</b>	8.93	<b>6.52</b>	6.91
	100%	10.89	10.72	10.86	<b>11.08</b>	<b>11.03</b>	<b>8.38</b>	9.13	<b>6.70</b>	7.28
Deutan	20%	11.67	22.27	18.07	<b>5.44</b>	5.49	<b>4.68</b>	5.56	<b>4.22</b>	4.26
	40%	11.09	18.00	13.90	<b>7.38</b>	<b>7.01</b>	<b>5.90</b>	6.68	<b>5.16</b>	5.25
	60%	10.58	15.08	11.05	<b>8.43</b>	<b>8.23</b>	<b>6.67</b>	7.32	<b>5.68</b>	5.79
	80%	10.15	13.31	9.41	<b>8.74</b>	<b>8.67</b>	<b>6.89</b>	7.51	<b>5.81</b>	5.93
	100%	9.81	12.50	9.04	<b>8.80</b>	<b>8.78</b>	<b>6.87</b>	7.54	<b>5.75</b>	5.92

### B. Quantitative Evaluation

Given the requirements for contrast enhancement and naturalness preservation, quantitative metrics are applied to compare the results of the proposed method with those of the state-of-the-art methods [10], [16], [17]. In the quantitative experiments, eleven natural images that contain natural scenes, artificial objects, and paints are selected as input images. Although both dichromacy and any degree of anomalous trichromacy are our compensation targets, and while the proposed method can synthesize images adapted to any degree of CVD, five degrees of CVD are assumed for the experiment: 20%, 40%, 60%, 80%, and 100%. As an ablation study w.r.t.  $\alpha$ , the recoloring result of using  $\alpha$  is compared with the result without using  $\alpha$ , which is equivalent to setting  $\alpha = 1$ .

1) *Naturalness Preservation*: Zhu *et al.* [16], [17] evaluated the naturalness of the recoloring results by comparing the CVD simulation result of the recolored image with that of the original image. The same evaluation scheme was adopted in this study. The CVD simulation result of the original image is denoted as reference image  $I^r$ , and that of the recolored image is denoted as test image  $I^t$ . Evaluation of the images is performed with the simulation of the corresponding degree used to generate the resulting image. For the existing methods [10], [16], [17], the resulting image recolored for dichromats is used for all five CVD degrees.

We calculate the chromatic difference between the test image and reference image pixel wisely. This approach was also introduced in [17]. Similar to [17], we convert the images to the CIE L\*a\*b\* color space, and the loss of naturalness (NL) is calculated as follows:

$$NL(I^t, I^r) = \frac{1}{N} \sum_{i=1}^N \sqrt{(a_i^t - a_i^r)^2 + (b_i^t - b_i^r)^2}, \quad (22)$$

where  $a_i^t, a_i^r, b_i^t$ , and  $b_i^r$  are a\* and b\* components of the  $i$ th pixel in  $I^t$  and  $I^r$  in the CIE L\*a\*b\* space, respectively. The smaller the NL value is, the more naturalness that is preserved. Table I shows the average loss of naturalness for the eleven resulting images using each method.

2) *Contrast Enhancement*: Compared with the original image, the contrast in the CVD simulation result is attenuated. Therefore, the recoloring algorithms are aimed at enhancing the

contrast in the simulation result or restoring it to its original level. Either way, the simulation result of the recolored image must be compared with the original image. In [19], the contrast in the simulation result was evaluated using the term for contrast preservation rate (CPR) in [39], which is defined as follows:

$$CPR(I^t, I^r) = \frac{1}{N} \sum_{i=1}^N \frac{1}{n-1} \frac{\sum_{j=1}^n (p_j - \mu_{pi})(q_j - \mu_{qi}) + \varepsilon}{\sigma_{pi}^2 + \sigma_{qi}^2 + \varepsilon}, \quad (23)$$

where  $p_i$  and  $q_i$  are corresponding pixels in the test image and reference image;  $p_j$  and  $q_j$  denote the neighboring pixels of  $p_i$  and  $q_i$ ;  $n$  denotes the number of neighboring pixels;  $\varepsilon$  is a small constant so that the denominator does not reach zero; and  $\mu_{pi}, \mu_{qi}, \sigma_{pi}$ , and  $\sigma_{qi}$  are the mean and standard deviation within the neighborhood of  $p_i$  and  $q_i$ , respectively. The higher the CPR value is, the better the contrast is preserved. Differing from naturalness evaluation, the original image, rather than its CVD simulated image, is adopted as reference image  $I^r$  in CPR in (23). The CPR scores using the four methods are shown in Table II. Parameter  $\beta$  is empirically set to 0.1, 0.2, and 0.3. For each degree, the best and worst scores of “with  $\alpha$ ” and “without  $\alpha$ ” among the results for three different  $\beta$  values are marked in red and blue, respectively. For each  $\beta$  value, the better value between “with  $\alpha$ ” and “without  $\alpha$ ” is in bold font. Since  $\beta$  is the weight of naturalness, the result of  $\beta = 0.3$  obtained the best naturalness score but worst contrast score among the three cases of  $\beta$ , while the result of  $\beta = 0.1$ , whose naturalness score is the worst, has the best score for contrast enhancement. In Table II, the result of “with  $\alpha$ ” has a better score of contrast enhancement than that of “without  $\alpha$ ” for all three  $\beta$  values. Compared to the existing methods, the proposed method, either “with  $\alpha$ ” or “without  $\alpha$ ,” achieved better scores for both naturalness and contrast in most cases. As the degree of CVD becomes milder, the superiority of the proposed method becomes more notable.

### C. Subjective Evaluation

To further clarify the performance of the proposed method, 14 CVD subjects (4 with a protan defect and 10 with a deutan defect) between the ages of 19 and 57 were recruited. Initially, we used the same subjective evaluation scheme as [16], [17], where participants were asked to estimate the naturalness of and amount of information in the images. However, the participants



TABLE II

AVERAGE CONTRAST PRESERVATION RATE SCORES OF ELEVEN RESULTING IMAGES SYNTHESIZED BY FOUR METHODS AND EVALUATED WITH SIMULATIONS OF CVD 20%, 40%, 60%, 80%, AND 100%. (A HIGHER VALUE INDICATES A BETTER RESULT)

Type	Degree	Hassan [10]	Zhu [16]	Zhu [17]	Proposed Method					
					$\beta=0.1$		$\beta=0.2$		$\beta=0.3$	
					Without $\alpha$	With $\alpha$	Without $\alpha$	With $\alpha$	Without $\alpha$	With $\alpha$
Protan	20%	0.973	0.777	0.877	0.973	<b>0.975</b>	<b>0.974</b>	0.974	0.975	<b>0.975</b>
	40%	0.931	0.812	0.879	0.939	<b>0.945</b>	0.942	<b>0.944</b>	0.942	<b>0.944</b>
	60%	0.891	0.836	0.881	0.908	<b>0.920</b>	0.908	<b>0.917</b>	0.907	<b>0.913</b>
	80%	0.868	0.850	0.883	0.889	<b>0.912</b>	0.886	<b>0.902</b>	0.883	<b>0.896</b>
	100%	0.865	0.855	0.884	0.879	<b>0.910</b>	0.873	<b>0.896</b>	0.872	<b>0.887</b>
Deutan	20%	0.967	0.914	0.877	0.974	<b>0.976</b>	<b>0.976</b>	0.975	0.976	<b>0.976</b>
	40%	0.930	0.899	0.878	0.947	<b>0.951</b>	0.949	<b>0.951</b>	0.949	<b>0.950</b>
	60%	0.897	0.880	0.880	0.923	<b>0.930</b>	0.923	<b>0.929</b>	0.923	<b>0.927</b>
	80%	0.877	0.865	0.881	0.909	<b>0.920</b>	0.907	<b>0.916</b>	0.906	<b>0.913</b>
	100%	0.869	0.856	0.881	0.903	<b>0.918</b>	0.900	<b>0.911</b>	0.898	<b>0.907</b>

TABLE III

THE COLOR VISION TEST RESULTS OF FOURTEEN PARTICIPANTS

Subject ID	Ishihara Test	Panel D15 Test	100-hue Test
P01	Protan	Normal	224
P02	Protan	Normal	240
P03	Protan	Protan	116
P04	Protan	Protan	192
D01	Deutan	Normal	104
D02	Deutan	Normal	140
D03	Deutan	Normal	196
D04	Deutan	Deutan	124
D05	Deutan	Deutan	196
D06	Deutan	Deutan	268
D07	Deutan	Deutan	272
D08	Deutan	Deutan	308
D09	Deutan	Deutan	384
D10	Deutan	Deutan	392

TABLE IV

RATIO OF IMAGES EVALUATED AS “PREFERABLE” BY THE FOURTEEN CVD PARTICIPANTS (A HIGHER VALUE INDICATES A BETTER RESULT)

Subject ID	Hassan [10]	Zhu [16]	Zhu [17]	Proposed Method					
				20%	40%	60%	80%	100%	
P01	0.27	0.09	0.09	<b>0.91</b>	0.82	0.82	0.82	<b>0.91</b>	
P02	0.36	0.27	0.27	<b>0.82</b>	<b>0.82</b>	0.73	0.64	0.64	
P03	0.27	0.45	0.45	0.91	<b>1.00</b>	0.91	0.91	0.82	
P04	0.64	0.64	0.82	<b>0.91</b>	<b>0.91</b>	0.73	0.64	0.73	
D01	0.55	0.36	0.00	<b>0.91</b>	0.82	0.82	0.82	0.82	
D02	0.36	0.18	0.18	<b>0.82</b>	0.64	0.64	0.64	0.64	
D03	0.27	0.18	0.09	<b>0.73</b>	0.64	0.64	0.64	0.55	
D04	0.45	0.36	0.45	<b>1.00</b>	<b>1.00</b>	0.91	0.82	0.73	
D05	0.09	0.18	0.64	0.91	<b>1.00</b>	0.82	0.73	0.64	
D06	0.00	0.27	<b>0.45</b>	0.36	<b>0.45</b>	0.36	<b>0.45</b>	0.36	
D07	0.18	0.36	0.73	<b>1.00</b>	<b>1.00</b>	0.91	<b>1.00</b>	0.82	
D08	0.18	0.09	0.55	0.55	0.73	<b>0.91</b>	0.73	0.73	
D09	0.36	0.27	0.36	<b>0.73</b>	0.64	0.64	0.55	0.64	
D10	0.82	0.73	0.91	<b>1.00</b>	<b>1.00</b>	<b>1.00</b>	<b>1.00</b>	<b>1.00</b>	

reported that 1) the definition of “naturalness” was confusing, and the images were scored according to their preference regarding the tint of the images; 2) it is not easy to evaluate the natural images from the perspective of information, as the information contained in natural images is very complex and the evaluation criteria are not simple. Based on these comments, in this study, the participants were asked to evaluate the natural images according to their preferences regarding the tint of the images. In addition, a much simpler task related to the Ishihara test was designed as an alternative to the information evaluation.

Before the participants were presented with the images, the Ishihara and Panel D15 tests were performed for type classification, the 100-hue test was performed for a degree check, and the results of the color vision test are shown in Table III. The participants are grouped by CVD type and are enumerated from “P01” to “D10” in ascending order based on the 100-hue test (Protan: “P01” to “P04,” Deutan: “D01” to “D10”). Since the Panel D15 test suggests that examinees who sort color caps in the “normal” order have a mild CVD defect, we enumerated such participants (“P01”, “P02”, and “D01” to “D03”) with smaller numbers than those who sorted in “protan” or “deutan” orders. The images were presented on an Iiyama ProLite 23-inch screen calibrated with X-Rite i1Display 2. During the experiment, participants sat half a meter away from the screen. An experiment with one participant lasted approximately two hours.

1) *Preference*: The participants evaluated the natural images that were introduced in the quantitative experiment. As the results compromise between naturalness and contrast, the results

of “ $\beta = 0.2$ , with  $\alpha$ ” were used for the evaluation. For each input image, eight resulting images, corresponding to the results of [10], [16], [17], and the proposed method for five different CVD degrees, were deemed as one test image set, and eleven sets were prepared in total. During the experiment, only one set at a time was presented to the participants, and the eight images were presented in random positions. Regarding preference, absolute-ness (whether or not the image is preferable) and relativeness (which one is more preferable) were simultaneously evaluated. For relative preference, all of the images were sorted according to the preference order. That is, the most preferable image was marked as “1st” and the least preferable as “8th.” For absolute preference, the participants were asked to mark the images that were preferable. Of course, the participants were allowed to mark none if none of the presented images were preferable.

The evaluation results for absolute preference and relative preference are shown in Table IV and Table V, respectively. The results of each participant are shown individually.

In Table IV, the score of a method is the absolute preferable rate (APR), which is calculated as follows:

$$APR(m) = \frac{APN(m)}{TN(m)} \quad (24)$$

where  $m$  refers to a recoloring method;  $TN(m)$  stands for the total number of resulting images generated with  $m$ , and  $APN(m)$

TABLE V  
AVERAGE PREFERENCE ORDER OF IMAGES EVALUATED BY THE FOURTEEN  
CVD PARTICIPANTS (A LOWER VALUE INDICATES A BETTER RESULT)

Subject ID	Hassan [10]	Zhu [16]	Zhu [17]	Proposed Method				
				20%	40%	60%	80%	100%
P01	6.00	7.09	6.91	2.27	<b>2.18</b>	3.55	3.64	4.36
P02	5.18	6.45	5.82	<b>2.82</b>	3.09	3.27	4.55	4.82
P03	6.18	5.82	5.82	<b>2.82</b>	3.18	3.82	4.00	4.36
P04	4.18	4.73	5.36	<b>3.09</b>	3.55	4.73	5.27	5.09
D01	4.36	5.82	7.73	<b>3.00</b>	3.18	3.36	4.45	4.09
D02	4.82	6.27	6.36	<b>3.27</b>	4.09	3.45	3.91	3.82
D03	5.27	6.36	6.73	<b>3.00</b>	3.27	3.36	3.82	4.18
D04	5.64	5.36	5.55	<b>3.45</b>	3.91	3.82	3.91	4.36
D05	7.18	6.55	3.82	<b>3.09</b>	3.73	<b>3.09</b>	4.00	4.55
D06	7.18	5.45	4.55	4.55	<b>3.00</b>	4.18	3.36	3.73
D07	6.82	6.18	3.73	3.73	<b>3.27</b>	3.91	4.00	4.36
D08	6.27	7.18	4.82	<b>3.27</b>	3.45	3.45	3.64	3.91
D09	5.09	5.82	5.00	4.18	3.82	<b>3.36</b>	4.09	4.64
D10	5.82	6.36	4.73	4.00	3.73	<b>3.18</b>	3.73	4.45

denotes the number of images that received a “preferable” label in  $TN(m)$ . In the table, the best score among the methods is highlighted in bold. Table IV shows that most participants evaluated that the results of our method with all assumed degrees are higher than those of all existing methods [10], [16], [17]. With the proposed method, a tendency can be observed that the score descends as the CVD degree ascends. In Table V, the score of a method is the average order of preference. Contrary to the scores in Table IV, the smaller the value is, the more preferable it is. Similar to the result of the absolute preference evaluation, the result of the relative evaluation shows that the images recolored by the proposed method obtained the best score. For the proposed method, the effect of naturalness preservation decreases when the assumed degree of deficiency increases. Therefore, it is important to choose a degree that is as mild as possible from the perspective of naturalness preservation.

2) *Discriminability*: Influenced by variations in the color gamut, the color perception of CVD individuals of the color distance is different from that of individuals with normal vision. For red–green CVD, reddish colors may become difficult to distinguish from greenish colors. In the Ishihara test, for example, individuals with normal vision have no difficulty reading figures constructed by reddish dots on a background with greenish dots, while those with CVD cannot read them because of reduced color discriminability. Therefore, the Ishihara test can be used to predict whether an individual has red–green CVD. In our experiment, we tested whether the participants could successfully read figures in the recolored images, which they failed to read with the original test charts. The participants were asked to directly illustrate the figures or lines on the presented test chart. Ten original test charts were selected from the Ishihara test. Together with the recolored charts, which were synthesized using existing methods and the proposed method, each participant was presented with 90 test charts (10 origins, 80 recoloring results) for evaluation. During the experiment, only one chart was presented on the screen at a time, and the order was random. Fig. 6 shows an example of the experimental results involving subjects “D04” and “D06.” Both “D04” and “D06” failed to read

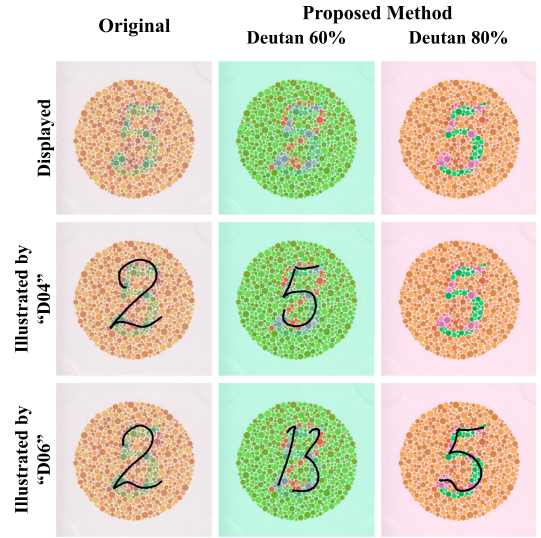


Fig. 6. Example of illustrations by two CVD subjects involved in the discriminability experiment. The black lines on the test charts are the illustrations by the subjects.

TABLE VI  
THE NUMBER OF CHARTS SUCCESSFULLY READ BY THE FOURTEEN CVD  
PARTICIPANTS AMONG NINE TEST CHARTS (A HIGHER VALUE INDICATES A  
BETTER RESULT)

Subject ID	Input	Hassan [10]	Zhu [16]	Zhu [17]	Proposed Method				
					20%	40%	60%	80%	100%
P01	3	3	0	4	7**	6	7	<b>10**</b>	9
P02	0	2	0	2	0	0	6***	8*	<b>9</b>
P03	0	2	1	2	0	1	6***	<b>8</b>	<b>8</b>
P04	1	1	2	2	1	2	5*	9**	8
D01	8	7	9	2	<b>10*</b>	<b>10</b>	<b>10</b>	<b>10</b>	7**
D02	2	2	3	2	5**	4	4	6	<b>7</b>
D03	1	2	1	1	0	2*	6**	<b>8</b>	<b>8</b>
D04	0	2	1	3	1	4**	8**	8	<b>9</b>
D05	0	1	1	2	2*	5**	8**	<b>9</b>	<b>9</b>
D06	0	1	0	1	0	1	2	5**	<b>5</b>
D07	0	2	0	3	1	4**	4	7**	<b>9*</b>
D08	0	2	0	1	1	2	5*	8*	7
D09	0	1	0	1	0	5***	5	8*	7
D10	0	0	0	1	0	2*	5*	6	<b>7</b>
Average	1.1	2.0	1.3	1.9	2.0	3.4	5.8	<b>7.9</b>	7.8

the figure “5” from the original chart. However, “D04” successfully read it from the recolored images with degrees 60% of the proposed method, while “D06” succeeded with that of degree 80%.

The evaluation results are shown in Table VI. The values in Table VI indicate the number of charts that the participant successfully read. Higher values mean better methods. The discriminability performance was the worst with the input images. On average, the scores of all degrees with the proposed method were comparable to or better than those for the input images and existing methods [10], [16], [17]. The results of the proposed method for the five degrees show a tendency for the performances of most participants to ascend as the assumed degree of CVD increased. In other words, the results assuming higher degrees (e.g., degree 80%) tend to obtain better scores than those assuming a lower degree (e.g., 60%). Nevertheless, the results of

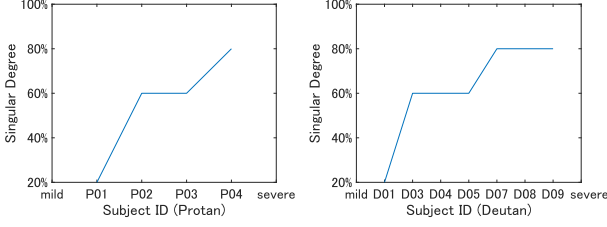


Fig. 7. Relationship between the CVD severity of participants and singular degrees.

five participants “P01,” “P04,” “D01,” “D08,” and “D09” show that the performances drop at 100% degree, which proves that recolored images for dichromacy are not always the best; in other words, it is necessary to adapt to the degrees to ensure optimal compensation. At the same time, the results of some degrees show significant improvements compared to those of the previous degrees, such as the results of degree 60% compared to 40% for “P02.” We assumed that such a significant improvement occurs for a degree correlated to the CVD degree of the participant. To verify this assumption, a one-tailed t-test with the null hypothesis that there is no significant difference between the discriminability scores of the proposed method for two adjacent degrees was applied to the performance of each participant; the results for degree 20% were compared to the input image. Each score was marked with “\*\*\*,” “\*\*,” or “\*” if the null hypothesis was rejected with a significance level of 0.01, 0.05, or 0.1, respectively. For the results of each participant, the lowest degree, with a above 5 and significantly higher than that of the previous degree, is named “singular degree” in this paper and is underlined in Table VI. We plot the CVD severities of the participants and their singular degrees indicated by the discrimination experiment in Fig. 7. For the participants with a protan defect, the singular degree increases gradually from “P01” to “P04” (a participant with a higher ID has more severe CVD). That is, a correlation exists between CVD severity and singular degree. This correlation can also be observed from “D01” to “D09,” who have a deutan defect. Although there are no clear singular degrees in “D02,” “D06,” and “D10,” the score of degree 20% evaluated by “D02” and that of degree 80% evaluated by “D06” are likely to be singular, which is in line with the ascending CVD severity of the participants shown in Fig. 7. This proves that the proposed method is adaptable to the degree of CVD.

The results of subject “D01,” who was diagnosed with mild CVD based on the 100-hue test and interview, show that the participant preferred the recolored images to a mild degree. Moreover, the results of subjects “D01” show that charts recolored with  $T = 20\%$  obtained the highest score. The proposed method provides sufficient contrast while simultaneously preserving naturalness, especially for individuals with mild CVD.

Interpreting the results from Table IV, Table V, and Table VI, if a higher CVD degree is assumed, then readability will usually improve as naturalness drops. Moreover, readability performance becomes saturated after reaching a particular degree. Comprehensively considering discrimination and preference, it is important to choose a degree that is as mild as possible but still readable by individuals with CVD.

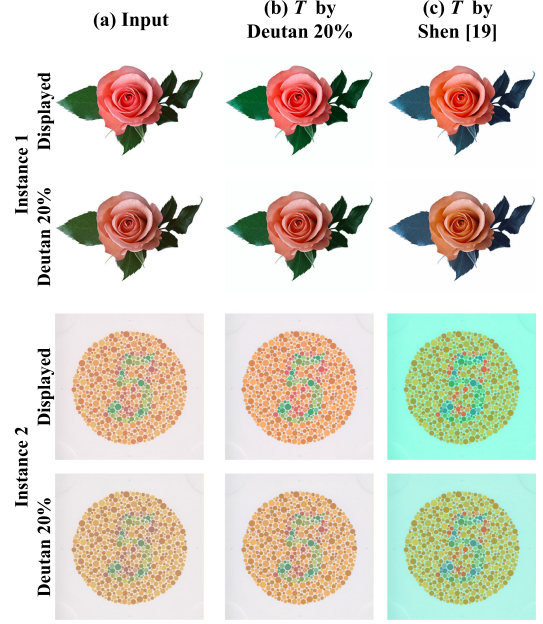


Fig. 8. Recoloring results of the proposed method when  $T$  is set as deutan 20% and set with Shen *et al.*’s calibration interface [19], respectively. Upper: images presented to the subject; lower: CVD simulation.

## V. DISCUSSION

### A. Selection of Transformation Matrix $T$

For practical usage, it is necessary to know the proper  $T$  for each individual CVD user. Currently, no method is available to accurately measure  $T$ . Shen *et al.* [19] developed a CVD calibration interface to predict the color transformation matrix  $T$  of CVD individuals. However, we found in experiments involving participants with a mild degree of CVD that the  $T$  given by [19] is likely to indicate a much more severe degree of CVD than the actual degree of the participants. This is not a major problem in most cases for the purpose of contrast enhancement, which is also the main purpose of [19]. However, as demonstrated by the experimental results, comprehensively considering discriminability and naturalness, it is important to choose a degree that is as mild as possible but still readable by individuals with CVD. Fig. 8 shows two results generated with the  $T$  given by [19]. Based on the 100-hue and Ishihara tests, the volunteer is diagnosed with mild deutan, and the predicted actual degree is approximately 20%. The volunteer reported a decreased preference for the image recolored with the  $T$  given by [19] (Instance 1) as well as decreased readability (Instance 2). For Instance 1, the color of the leaves was perceived to be green (Fig. 8(a)); however, as shown in Fig. 8(c), the leaves will be perceived as blue in the image recolored using  $T$  given by [19], and the participant indicated that such a change from the original image is not preferable. For Instance 2, both the figure and the dots in the background in Fig. 8(c) appear to be greenish, and the figure has become somewhat difficult to recognize. Nevertheless, as a CVD degree calibration tool, Shen *et al.* [19] provide an option for us. Although some additional calibration is necessary, the tool has high potential for being combined with our method to achieve



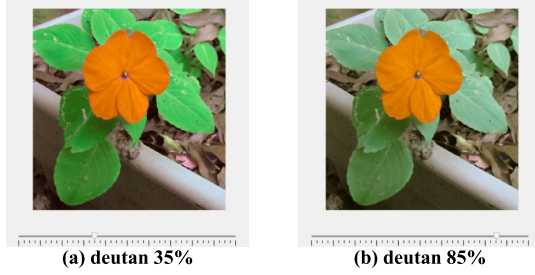


Fig. 9. Application for users to select an appropriate  $T$ . (a) When the user moves the scrollbar to 35%. (b) When the user moves the scrollbar to 85%.

TABLE VII

THE AVERAGE STRUCTURAL SIMILARITY SCORES OF 11 INTERPOLATED IMAGES OF DEGREES 10%, 30%, 50%, 70%, AND 90% COMPARED TO DIRECTLY GENERATED IMAGES

Degrees	10%	30%	50%	70%	90%
Protan	0.981	0.998	0.998	0.999	0.999
Deutan	0.982	0.998	0.999	0.998	0.999

TABLE VIII

THE AVERAGE FEATURE SIMILARITY COLOR SCORES OF 11 INTERPOLATED IMAGES OF DEGREES 10%, 30%, 50%, 70%, AND 90% COMPARED TO DIRECTLY GENERATED IMAGES

Degrees	10%	30%	50%	70%	90%
Protan	0.995	0.999	0.999	1.000	1.000
Deutan	0.995	0.999	0.999	1.000	1.000

the best recoloring effect. In this study, as shown in Fig. 9, we designed an interface for users to select the best image by interactively adjusting  $T$ . The interface contains a scrollbar that can be moved in “1%” units. Therefore, 100 images were required for the application. Although generating all these images offline can be considered a solution, as it takes 20 seconds to generate one image, which will be discussed in the following Section, it is still time-consuming to generate all 100 images. To save computation time, we generated several key images from  $T$  and then obtained the rest by linearly interpolating those key images. To clarify the feasibility of such a scheme, we evaluated the error from the results directly generated from  $T$  using SSIM [39]. The original SSIM was extended to use all of three chromatic channels rather than only luminance channel. Furthermore, we evaluated the error with the extended FSIM color metric in [40]. The eleven natural scenery images used in the naturalness evaluation were adopted as test images. Table VII and Table VIII show the average SSIM scores and extended FSIM scores in the results for degrees 10%, 30%, 50%, 70%, and 90% using the results of degrees 20%, 40%, 60%, 80%, and 100% as the key images for interpolation. Table IX and Table X show the average SSIM scores and extended FSIM scores in the results of degrees 5%, 15%, ..., and 95% using the results of degrees 10%, 20%, ..., and 100% as the key images for interpolation. The evaluation results show high similarity between the interpolated images and directly generated images. Future work should explore the potential of using this application to easily obtain appropriate  $T$ , for example, by identifying the appropriate properties of the images to be used as the stimulus.

TABLE IX

THE AVERAGE STRUCTURAL SIMILARITY SCORES OF 11 INTERPOLATED IMAGES OF DEGREES 5%, 15%, 25%, 35%, 45%, 55%, 65%, 75%, 85%, AND 95% COMPARED TO DIRECTLY GENERATED IMAGES

Degrees	5%	15%	25%	35%	45%
Protan	0.981	0.998	0.999	0.999	0.997
Deutan	0.981	0.997	0.996	0.999	0.999
Degrees	55%	65%	75%	85%	95%
Protan	0.998	0.998	0.997	0.999	0.999
Deutan	0.999	0.997	0.999	0.998	0.998

TABLE X

THE AVERAGE FEATURE SIMILARITY COLOR SCORES OF 11 INTERPOLATED IMAGES OF DEGREES 5%, 15%, 25%, 35%, 45%, 55%, 65%, 75%, 85%, AND 95% COMPARED TO DIRECTLY GENERATED IMAGES

Degrees	5%	15%	25%	35%	45%
Protan	0.997	0.998	1.000	1.000	0.999
Deutan	0.996	0.998	0.999	1.000	1.000
Degrees	55%	65%	75%	85%	95%
Protan	1.000	1.000	1.000	1.000	1.000
Deutan	0.999	0.999	1.000	0.999	1.000

TABLE XI

AVERAGE TIME COST OF THE PROPOSED METHOD WITH THREE EDIT PROPAGATION BACKENDS WITH AN AVERAGE PIXEL NUMBER OF 179 k

Procedure	Extract	Recolor	Propagation			Total
			Backend	Processor	Time	
Time: (s)	7.08	0.04	[36]	CPU	116.26	123.38
				GPU	11.69	18.81
			[37]	CPU	7.87	14.99
				CPU	13.68	20.80

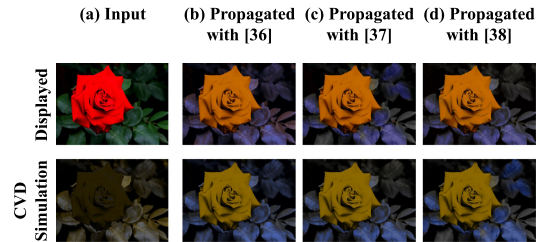


Fig. 10. Comparison of propagation results of Chen *et al.* [36], Li *et al.* [37], and Xu *et al.* [38].

## B. Computation Time

The proposed method is implemented on a PC with MATLAB 2020a, a 3.50 GHz AMD CPU, 64 GB of RAM, and TITAN RTX. The time efficiency of three procedures, dominant color extraction, recoloring, and propagation of the proposed method, is shown in Table XI. The average number of pixels of the test images is 179 k. As shown in the table, of the three edit propagation methods, all account for more than 50% of the total time; that is, the bottleneck of time efficiency is edit propagation. In particular, propagation with [36] on a CPU required 123.38 s, while the runtime could be reduced to 11.69 s on a GPU. The runtime of [37], [38] is also shown in Table XI. An example of the propagation results with [36], [37], and [38] is shown in Fig. 10. The size of the input image is  $680 \times 494$ . For the case shown in Fig. 10, it is hard to identify the differences between the results with the naked eye, and the CPU runtimes for [36] (Fig. 10(b)), [37] (Fig. 10(c)), and [38] (Fig. 10(d)) are 51.3 s,

3.1 s, and 20.2 s, respectively. For practical use, the implementation of the proposed method on mobile devices, such as smart phones, should be considered. Therefore, improving the time efficiency of the proposed method is essential and should be explored in future work.

### C. Further Improvements

Currently, we adopted the anomalous trichromats simulation model [22], which was built in RGB color space, and thereby, we implemented our work in RGB color space as well. Nevertheless, the proposed method can be easily transferred to other color perceptual space by strategies, for example, transferring the simulation model to CIE  $L^*a^*b^*$  color space by least square approximation, an approach adopted in [13]. For video applications, our method has high potential in producing effective and stable recoloring results by adding a temporal consistency preserving term to the objective function. Extending the proposed method to video will be an important focus of our future work. In our experiment, we listed the evaluation results assessed by participants and labeled the best score of each participant. However, further exploring the information inside these data using some mathematical tools, such as the pair comparison matrix, will also require future work.

## VI. CONCLUSION

This study proposed a degree-adaptable recoloring method that simultaneously enhances contrast and preserves naturalness to assist individuals with different degrees of CVD. A quantitative evaluation showed that the proposed method achieves better performance than the current state-of-the-art methods. A subjective evaluation showed that the proposed method could adaptively deal with individual differences in the requirements for contrast enhancement and naturalness preservation. In terms of the study's limitations, further improvements in time efficiency are required, especially when used in real applications with the interface introduced in Section 5. Potential future work could apply the proposed method to develop a user-friendly system for the accurate measurement of  $T$ .

## ACKNOWLEDGMENT

The authors would like to thank all the participants for evaluating the proposed method carefully and patiently and for their valuable comments. At the same time, we would like to thank the reviewers for their constructive comments and suggestions! We appreciate our project members, especially Mr. Ying Tang for the valuable discussions.

## REFERENCES

- [1] L. T. Sharpe, A. Stockman, H. Jägle, and J. Nathans, "Opsin genes, cone photopigments, color vision, and color blindness," *Color Vision: From Genes to Perception*, pp. 3–51, 1999.
- [2] J. Nam, Yong Man Ro, Y. Huh, and M. Kim, "Visual content adaptation according to user perception characteristics," *IEEE Trans. Multimedia*, vol. 7, no. 3, pp. 435–445, Jun. 2005.
- [3] J.-B. Huang, C.-S. Chen, T.-C. Jen, and S.-J. Wang, "Image recolorization for the colorblind," in *Proc. IEEE Int. Conf. Acoust., Speech, Signal Process.*, 2009, pp. 1161–1164.
- [4] K. Rasche, R. Geist, and J. Westall, "Detail preserving reproduction of color images for monochromats and dichromats," *IEEE Comput. Graph. Appl.*, vol. 25, no. 3, pp. 22–30, May-Jun. 2005.
- [5] K. Rasche, R. Geist, and J. Westall, "Re-coloring images for gamuts of lower dimension," in *Comput. Graph. Forum*, vol. 24, Wiley Online Library, 2005, pp. 423–432.
- [6] K. Wakita and K. Shimamura, "SmartColor: Disambiguation framework for the colorblind," in *Proc. 7th ACM SIGACCESS Conf. Comput. Accessibility*, 2005, pp. 158–165.
- [7] G. M. Machado and M. M. Oliveira, "Real-time temporal-coherent color contrast enhancement for dichromats," in *Comput. Graph. Forum*, vol. 29, Wiley Online Library, 2010, pp. 933–942.
- [8] H.-Y. Lin, L.-Q. Chen, and M.-L. Wang, "Improving discrimination in color vision deficiency by image re-coloring," *Sensors*, vol. 19, no. 10, pp. 2250:1–2250:19, 2019.
- [9] M. F. Hassan and R. Paramesran, "Naturalness preserving image recoloring method for people with red-green deficiency," *Signal Process.: Image Commun.*, vol. 57, pp. 126–133, 2017.
- [10] M. F. Hassan, "Flexible color contrast enhancement method for red-green deficiency," *Multidimensional Syst. Signal Process.*, vol. 30, no. 4, pp. 1975–1989, 2019.
- [11] C. Lau, W. Heidrich, and R. Mantiuk, "Cluster-based color space optimizations," in *Proc. Int. Conf. Comput. Vis.*, 2011, pp. 1172–1179.
- [12] J.-B. Huang, Y.-C. Tseng, S.-I. Wu, and S.-J. Wang, "Information preserving color transformation for protanopia and deuteranopia," *IEEE Signal Process. Lett.*, vol. 14, no. 10, pp. 711–714, Oct. 2007.
- [13] G. R. Kuhn, M. M. Oliveira, and L. A. Fernandes, "An efficient naturalness-preserving image-recoloring method for dichromats," *IEEE Trans. Visualization Comput. Graph.*, vol. 14, no. 6, pp. 1747–1754, 2008.
- [14] C.-R. Huang, K.-C. Chiu, and C.-S. Chen, "Key color priority based image recoloring for dichromats," in *Proc. Pacific-Rim Conf. Multimedia*. Springer, 2010, pp. 637–647.
- [15] C. Huang, K. Chiu, and C. Chen, "Temporal color consistency-based video reproduction for dichromats," *IEEE Trans. Multimedia*, vol. 13, no. 5, pp. 950–960, Oct. 2011.
- [16] Z. Zhu, M. Toyoura, K. Go, I. Fujishiro, K. Kashiwagi, and X. Mao, "Processing images for red-green dichromats compensation via naturalness and information-preservation considered recoloring," *Vis. Comput.*, vol. 35, no. 6–8, pp. 1053–1066, 2019.
- [17] Z. Zhu, M. Toyoura, K. Go, I. Fujishiro, K. Kashiwagi, and X. Mao, "Naturalness and information-preserving image recoloring for red-green dichromats," *Signal Process.: Image Commun.*, vol. 76, pp. 68–80, 2019.
- [18] S. Hau Chua, H. Zhang, M. Hammad, S. Zhao, S. Goyal, and K. Singh, "Colorbliss: Augmenting visual information for colorblind people with binocular luster effect," *ACM Trans. Comput.-Hum. Interaction*, vol. 21, no. 6, pp. 32:1–32:20, 2015.
- [19] W. Shen, X. Mao, X. Hu, and T.-T. Wong, "Seamless visual sharing with color vision deficiencies," *ACM Trans. Graph.*, vol. 35, no. 4, pp. 70:1–70:12, 2016.
- [20] X. Hu, Z. Zhang, X. Liu, and T.-T. Wong, "Deep visual sharing with colorblind," *IEEE Trans. Comput. Imag.*, vol. 5, no. 4, pp. 649–659, Dec. 2019.
- [21] H. Xinghong, L. Xueting, Z. Zhuming, X. Menghan, L. Chengze, and W. Tien-Tsin, "Colorblind-shareable videos by synthesizing temporal-coherent polynomial coefficients," *ACM Trans. Graph.*, vol. 38, no. 6, pp. 174:1–174:12, 2019.
- [22] G. M. Machado, M. M. Oliveira, and L. A. Fernandes, "A physiologically-based model for simulation of color vision deficiency," *IEEE Trans. Visualization Comput. Graph.*, vol. 15, no. 6, pp. 1291–1298, Nov. -Dec. 2009.
- [23] H. Brettel, F. Viénot, and J. D. Mollon, "Computerized simulation of color appearance for dichromats," *JOSA A*, vol. 14, no. 10, pp. 2647–2655, 1997.
- [24] F. Viénot, H. Brettel, and J. D. Mollon, "Digital Video Colourmaps for Checking the Legibility of Displays by Dichromats," *Color Res. Appl.*, vol. 24, no. 4, pp. 243–252, 1999.
- [25] D. B. Judd, "Fundamental studies of color vision from 1860 to 1960," *Proc. the Nat. Acad. Sci. the United States America*, vol. 55, no. 6, pp. 1313–1330, 1966.
- [26] "Enchroma," [Online]. Available: <https://enchroma.com/>
- [27] "Vino," [Online]. Available: <https://www.vino.vi/>
- [28] L. Gómez-Robledo, E. Valero, R. Huertas, M. Martínez-Domingo, and J. Hernández-Andrés, "Do enchroma glasses improve color vision for colorblind subjects?," *Opt. Exp.*, vol. 26, no. 22, pp. 28693–28703, 2018.

- [29] M. A. Martínez-Domingo *et al.*, "Assessment of vino filters for correcting red-green color vision deficiency," *Opt. Exp.*, vol. 27, no. 13, pp. 17 954–17 967, 2019.
- [30] D. Arthur and S. Vassilvitskii, "k-means++: The advantages of careful seeding," *Proc. 18th ACM-SIAM Symp. Discrete Algorithms*, 2007, pp. 1027–1035.
- [31] P. Hung and N. Hiramatsu, "A colour conversion method which allows colourblind and normal-vision people share documents with colour content," *Konica Minolta Technol. Rep.*, vol. 10, no. 1, pp. 30–36, 2013.
- [32] B. Sajadi, A. Majumder, M. M. Oliveira, R. G. Schneider, and R. Raskar, "Using patterns to encode color information for dichromats," *IEEE Trans. Visualization Comput. Graph.*, vol. 19, no. 1, pp. 118–129, Jan. 2013.
- [33] S. Ishihara, *Test for Colour-Blindness*. Tokyo, Japan: Kanehara, 1987.
- [34] D. Farnsworth, *The Farnsworth Dichotomous Test for Color Blindness, Panel D-15: Manual*. New York, NY, USA: Psychological Corporation, 1947.
- [35] D. Farnsworth, "The farnsworth-munsell 100-hue and dichotomous tests for color vision," *JOSA*, vol. 33, no. 10, pp. 568–578, 1943.
- [36] X. Chen, D. Zou, Q. Zhao, and P. Tan, "Manifold preserving edit propagation," *ACM Trans. Graph.*, vol. 31, no. 6, pp. 132:1–132:7, 2012.
- [37] Y. Li, T. Ju, and S. Hu, "Instant propagation of sparse edits on images and videos," in *Proc. Conf. Comput. Graph. Forum*, vol. 29. Wiley Online Library, 2010, pp. 2049–2054.
- [38] L. Xu, Q. Yan, and J. Jia, "A sparse control model for image and video editing," *ACM Trans. Graph.*, vol. 32, no. 6, pp. 197:1–197:10, 2013.
- [39] Z. Wang, A. C. Bovik, H. R. Sheikh, and E. P. Simoncelli, "Image quality assessment: From error visibility to structural similarity," *IEEE Trans. Image Process.*, vol. 13, no. 4, pp. 600–612, Apr. 2004.
- [40] L. Zhang, L. Zhang, X. Mou, and D. Zhang, "FSIM: A feature similarity index for image quality assessment," *IEEE Trans. Image Process.*, vol. 20, no. 8, pp. 2378–2386, Aug. 2011.



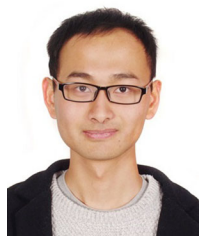
researches.

**Kenji Kashiwagi** received the M.D. and Ph.D. degrees from the University of Yamanashi, Kofu, Japan. He is currently a Professor with the Department of Ophthalmology, Faculty of Medicine, University of Yamanashi. He is also a Clinical Scientist in the field of ophthalmology, especially glaucoma. His research interests include not only clinical but also basic science and he is currently working on some subjects with a variety of experts both inside and outside of the University of Yamanashi. He has received several domestic and international awards for his

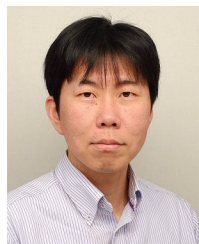


Associate Editor for the IEEE TVCG and Elsevier *Journal of Visual Informatics*. He is an Honorary Member of the IEEE, a Fellow of the JFES, a Senior Member of the ACM and IPSJ, and a Member of Science Council of Japan.

**Issei Fujishiro** (Senior Member, IEEE) received the Doctor of Science degree in information sciences from The University of Tokyo, Tokyo, Japan, in 1988. He is currently a Professor with the Center for Information and Computer Science, Graduate School of Science and Technology, Keio University, Tokyo, Japan. His research interests include graphical modeling paradigms, applied visualization design, and smart multimodal ambient media. He is on the Steering Committee for the IEEE PacificVis and the Area Model Curation Committee for the IEEE VIS and an



**Zhenyang Zhu** received the B.S. degree in computer science from Zhejiang Gongshang University, Hangzhou, China, in 2016 and the M.S. degree in 2018 in computer science from the University of Yamanashi, Kofu, Japan, where he is currently working toward the doctorate degree with the Graduate School of Engineering. His research interests include computer graphics, image processing, and human-computer interaction.



**Masahiro Toyoura** (Member, IEEE) received the B.Sc. degree in engineering, and the M.Sc. and Ph.D. degrees in informatics from Kyoto University, Kyoto, Japan, in 2003, 2005, and 2008, respectively. He is currently an Associate Professor with the Department of Computer Science and Engineering, University of Yamanashi, Kofu, Japan. His research interests include digital fabrication, computer vision, and augmented reality.



Institute and State University, Blacksburg, VA, USA. His current research interests include human-centered design, user experience design, human-computer interaction, and telemedicine.

**Kentaro Go** received the B.E. degree in electrical engineering from the University of Yamanashi, Kofu, Japan, and the M.S. degree in information engineering and the Ph.D. degree in information sciences from Tohoku University, Sendai, Japan. He is currently a Professor with the Department of Computer Science and Engineering, University of Yamanashi. He was a Research Associate with the Research Institute of Electrical Communication, Tohoku University and a Postdoctoral Researcher with the Center for Human-Computer Interaction, Virginia Polytechnic



University, Blacksburg, VA, USA. His current research interests include human-centered design, user experience design, human-computer interaction, and telemedicine.

**Tien-Tsin Wong** (Member, IEEE) received the B.Sc., M.Phil., and Ph.D. degrees in computer science from The Chinese University of Hong Kong, Hong Kong, in 1992, 1994, and 1998, respectively. In August 1999, he joined the Computer Science & Engineering Department, The Chinese University of Hong Kong. He is currently a Professor. He is also a Core Member with the Virtual Reality, Visualization, and Imaging Research Centre, The Chinese University of Hong Kong. His main research interests include computer graphics, computer vision, machine learning, computational manga, precomputed lighting, image-based rendering, GPU techniques, medical visualization, and multimedia compression. He was the recipient of the IEEE TRANSACTIONS ON MULTIMEDIA Prize Paper Award 2005 and the Young Researcher Award 2004.



virtual and augmented reality, and their applications to e-health. She is a Member of ACM and is an Associate Editor for *The Visual Computer*. She was the receipt of the Computer Graphics International 2018 Achievement Award.

**Xiaoyang Mao** (Member, IEEE) received the B.S. degree in computer science from Fudan University, Shanghai, China, and the M.S. and Ph.D. degrees in computer science from The University of Tokyo, Tokyo, Japan. She is currently a Professor with the Department of Computer Science and Engineering, University of Yamanashi, Kofu, Japan and an Adjunct Professor with the School of Computer Science and Technology, Hangzhou Dianzi University, Hangzhou, China. Her research interests include image processing, visual perception, non-photorealistic rendering,